

PAPER • OPEN ACCESS

Numerical Modelling of a Fast Pyrolysis Process in a Bubbling Fluidized Bed Reactor

To cite this article: S Jalalifar *et al* 2017 *IOP Conf. Ser.: Earth Environ. Sci.* **73** 012032

View the [article online](#) for updates and enhancements.

Related content

- [Oxidative Pyrolysis of Agricultural Residues in Gasification and Carbonization Processes](#)
Xuan-Huynh Pham, Laurent Van De Steene, Bruno Piriou *et al.*
- [Modeling Lab-sized Anaerobic Fluidized Bed Reactor \(AFBR\) for Palm Oil Mill Effluent \(POME\) treatment: from Batch to Continuous Reactors](#)
Muhammad Mufti Azis, Hanifrahmawan Sudibyo and Wiratni Budhijanto
- [Ammonium Removal Efficiency in Fixed Bed Reactor and Suspended Growth Reactor Using Ecotru Inoculation](#)
Rusyda Syahidah, Sudarno and Badrus Zaman



IOP | ebooks™

Bringing you innovative digital publishing with leading voices to create your essential collection of books in STEM research.

Start exploring the collection - download the first chapter of every title for free.

Numerical Modelling of a Fast Pyrolysis Process in a Bubbling Fluidized Bed Reactor

S Jalalifar¹, M Ghiji¹, R Abbassi¹, V Garaniya¹, and K Hawboldt²

¹ Australian Maritime College, National Centre of Maritime Engineering and Hydrodynamics, University of Tasmania, Launceston, Tasmania, Australia.

² Faculty of Engineering and applied Science, Memorial University, St. John's, NL, Canada.

E-mails: salman.jalalifar@utas.edu.au;

Abstract. In this study, the Eulerian-Granular approach is applied to simulate a fast pyrolysis bubbling fluidized bed reactor. Fast pyrolysis converts biomass to bio-products through thermochemical conversion in absence of oxygen. The aim of this study is to employ a numerical framework for simulation of the fast pyrolysis process and extend this to more complex reactor geometries. The framework first needs to be validated and this was accomplished by modelling a lab-scale pyrolysis fluidized bed reactor in 2-D and comparing with published data. A multi-phase CFD model has been employed to obtain clearer insights into the physical phenomena associated with flow dynamics and heat transfer, and by extension the impact on reaction rates. Biomass thermally decomposes to solid, condensable and non-condensable and therefore a multi-fluid model is used. A simplified reaction model is used where the many components are grouped into a solid reacting phase, condensable/non-condensable phase, and non-reacting solid phase (the heat carrier). The biomass decomposition is simplified to four reaction mechanisms based on the thermal decomposition of cellulose. A time-splitting method is used for coupling of multi-fluid model and reaction rates. A good agreement is witnessed in the products yield between the CFD simulation and the experiment.

1. Introduction

Concern about limited supply of fossil fuels and environmental risks such as global warming and climate change is a strong motivation for development of environmentally friendly technologies and renewable energy sources. Biomass is abundant and therefore an alternative energy source. All organic materials such as plants (byproduct and residue of agricultural products) and animal resources (available in land and water environments) can be classified as biomass. Agricultural waste such as corn stover, bagasse and residues associated with harvesting crops contain high-energy organics in the form of cellulose, hemicellulose, and lignin. Compared to conventional fossil fuels, energy derived from biomass has lower emissions of sulfur dioxides (SO₂) and particulate matter (PM). In addition, energy from biomass is considered carbon neutral because the released carbon dioxide (CO₂) into the environment is recycled by the photosynthesis process. The quality of energy derived from biomass can be improved by conversion to a liquid or more homogenous solid. Thermochemical conversions are mainly: direct combustion of biomass to provide heat; gasification to produce gas as a synthesis gas, heat, and/or power; pyrolysis to generate bio-oil, char, and gas [1].

Pyrolysis offers the advantage of producing three bioproducts; a bio-oil for liquid fuel or source of high value chemicals; a solid biochar (e.g. sustainable source for adsorbent, soil amendment, or catalyst); and a biogas for energy recovery. Pyrolysis is loosely divided into three different categories; slow, fast, and flash pyrolysis. The primary product of slow pyrolysis is the char, and for fast and flash pyrolysis, the primary product is the liquids. Extracted bio-oil from biomass and can be consumed



directly for the generation of heat and power in boilers, gas turbines, and diesel engines, or it can be refined to produce a higher quality fuel [2, 3].

Fast pyrolysis has been studied for a variety of biomass feedstock, types of reactors, and operating conditions. The reaction mechanisms are complex due to the heterogeneity of the biomass and the number of phases, however some researchers have studied global and intrinsic reaction rates [4, 5]. The drawback to detailed reaction mechanisms is that they are specific to a feedstock and operating conditions and difficult to determine completely due to the multiple reactions occurring in the various phases and the ability to accurately measure the products. Typically, series of global reactions are assumed where the biomass is converted through a series of primary and secondary reactions [6]. The reaction rates are typically derived in reactors where heat and mass transfer resistances are minimized. To properly model a pilot or commercial scale reactor these resistances must be included in the form of transport equations. Physical phenomena such as flow dynamics (multi-phase flow and mechanically moving parts), phase equilibrium, and heat and mass transfer, can be modelled and predicted by means of Computational Fluid Dynamics (CFD) modelling techniques. The reaction rates can be included in the CFD model.

The widespread applications of fluidized bed reactors have motivated many researchers to use CFD techniques to obtain a better understanding of the reactor transport phenomena. Parameters involved in the simulation include; pyrolysis temperature, the size of biomass particles, biomass feed rate, residence time and carrier gas velocity. Temperature and residence time of the condensable and non-condensable gases determine largely the amount of tar (bio-oil) produced. Temperatures exceeding 550-600 °C and longer vapour residence times (e.g. lower nitrogen flow rates) will result in secondary cracking reactions, which decrease yield of the tar and increase the water content [6]. One method to vary the residence times in fluidized beds is to vary the location of the biomass feed relative to the reactor height [7]. The biomass feed rate is a factor in solid particle residence time, there is a balance between minimizing secondary reactions and ensuring the biomass particles are well mixed and reach thermal equilibrium [8]. The carrier gas (typically nitrogen) velocity must be higher than the minimum fluidization velocity to maintain fluidization conditions and ensure the biomass and sand are well mixed to maximize heat transfer. However, if nitrogen flow rates become too high sand may become entrained in the exit gases/char. The biomass particle size determines the heating rate of the particle and ideally, fine particles are used to minimize intraparticle heat and mass transfer resistances. However, there is a balance between minimum particle size and costs to grind to this size.

2. Methodology

2.1. Chemical kinetics of a single particle

In this study, a combination of the Bradbury et al. [9] model of cellulose to “active material” which then reacts to tar and char is employed. The tar then further reacts to form gas. As illustrated in figure 1, three different phases including biomass phase, sand phase and gas phase are taken into account. Each phase involved in the process has a number of species. The biomass phase includes unreacted biomass and char, while the gas phase include condensable (tar), non-condensable and the nitrogen. The sand phase and nitrogen are inert and do not participate in the chemical reactions. The reaction rate constants are calculated as below:

$$k_i = A_i \exp[-Ea_i / (RT)] \quad (1)$$

Where k_i is the rate constant for reaction “ i ”, and A_i and Ea_i are the associated Arrhenius constant and activation energies. “ T ” is the temperature in kelvin and “ R ” is the gas constant. As indicated previously, overall seven different groups are included in this reaction scheme the solid reaction phase (virgin cellulose, active cellulose, and biochar), the condensable/non-condensable phase, and the non-reacting sand phase. The nitrogen is included in the gas phase as it contributes to partial pressures but does not react. The values of the kinetic parameters for the reaction scheme and the obtained values for heats of reaction of cellulose are outlined in Table 1. Y is the formation ratio for the char component, which is 0.35 for pyrolysis of pure cellulose [10].

2.2. Mathematical methods/models

The fundamental governing equations are the conservation of mass, momentum, energy, and species. Thus, a combination of Multi Fluid Model (MFM) and a chemical solver is the most appropriate method to simulate biomass fast pyrolysis. In multi-fluid model, all phases are treated as continua. For the solution of the governing equations, the Kinetic Theory of Granular Flow (KTFG) [11] is applied to for the solid phases. Further details about the description of the models can be found in the literature [7]. Numerical models and settings.

The multiphase fluid flow, heat transfer, chemical reactions, and species mass transfer in the lab-scale fluidized bed reactor is simulated using the solver FLUENT16.0. The dimensions of the reactor are outlined in figure 2. The laminar multiphase Eulerian-Granular flow is used and the energy equations and species transport are activated. The first fractional step considers merely the spatial solution of the multiphase species with the reaction terms set to zero. In the next fractional step, the reaction terms are integrated in each cell using a stiff ODE solver. Time discretization was done using a second-order implicit method. The pressure-based solver used a least-square cell based phase coupled SIMPLE-algorithm for the pressure velocity coupling and second order (upwind) discretization was applied for the momentum, energy and species modelling parameters. QUICK algorithm is applied for volume fraction calculations. Finally, hybrid initialization is applied and each phases; especially the sand phase; are patched based on the initial packing limit.

2.2.1. Computational domain, initial and boundary conditions

The 2-D computational domain is shown in figure 2. Biomass with diameter of 0.4 mm at an inlet temperature of 300 K is fed at a rate of 100 g/h. Nitrogen flows from the bottom of the bed at a velocity of 0.36 m/s and temperature 773 K. The sand with diameter of 0.52 mm is initially packed to the height of 5.5 cm with the volume fraction of 0.59. The outflow boundary condition is used at the outlet. No-slip wall condition is applied for the solid walls. To simulate external heating, the wall temperature is kept constant at of 773 K. The bed temperature is initially set to 773 K. The biomass feedstock of pure cellulose. A study conducted for the grid independence shows that a 2-D grid with 2055 quadrilateral cells is capable of predicting all parameters to an acceptable level of accuracy. To avoid numerical instability small time step size of 1×10^{-4} s is used at the commencement of the simulation. However the grid resolution adopted here allow us to opt for the maximum time step size of 5×10^{-4} s without any numerical instability. In the solution of species transport equations, mass fraction of each species must sum to unity. Therefore, the N_{th} mass fraction is determined as one minus the sum of the N-1 solved mass fractions. To minimize numerical error, the N_{th} species should be selected as that species with the overall largest mass fraction (nitrogen in the gas phase and cellulose in the biomass phase). The thermo-physical properties of species involved in the reactions of the biomass are given in Table 2. It is worth noting that incompressible ideal gas model calculates the density of gaseous species and the viscosity of the solid species are calculated based on granular models.

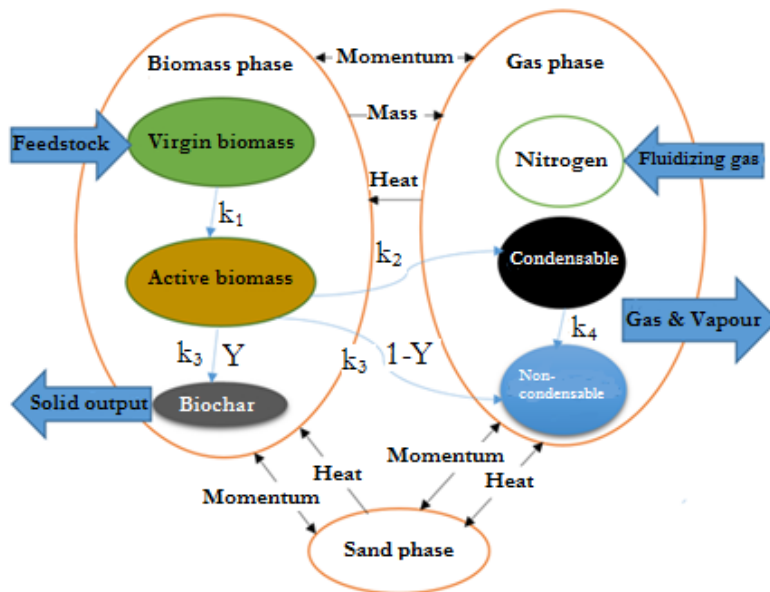


Figure 1. Chemical reactions and exchange of mass, momentum, and heat between phases.

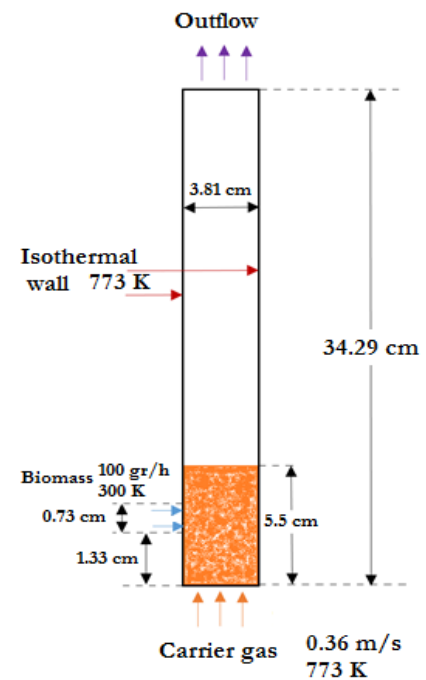


Figure 2. Schematic geometry of 2-D model of bubbling fluidized bed for simulations.

Table 1. Pre-exponential factor and activation energies for the biomass component [10].

Components	Reaction	A(s-1)	E(MJ/kmol)	Heat release, ΔH (kJ/kg)
Cellulose	k_1	2.8×10^{19}	242.4	0
	k_2	3.28×10^{14}	196.5	255
	k_3	1.3×10^{10}	150.5	-20
Tar	k_4	4.25×10^6	108.0	-42

Table 2. Thermo-physical properties of species [12]

Species	Density ρ (kg/m ³)	Particle diameter d_p (m)	Molecular weight (g/mol)	Heat capacity C_p (J/kg K)	Dynamic viscosity μ (kg/ms)	Thermal conductivity k (J/kg K)
Tar	-	-	100	2500	3×10^{-5}	2.577×10^{-2}
Gas	-	-	30	1100	3×10^{-5}	5.63×10^{-2}
N ₂	-	-	28	1121	3.58×10^{-5}	2.577×10^{-2}
Cellulose	400	4×10^{-4}	12.14	2300	-	0.3
Biochar	2333	4×10^{-4}	12.01	1100	-	0.1
Sand	2649	5.2×10^{-4}	60.08	800	-	0.27

3. Results and discussions

A grid dependence study is carried out using 2-D mesh with four different mesh resolutions. The number of meshes for cases 1-4 are 225, 910, 2055, and 3640, respectively. The temperature distribution from the centreline of the reactor is shown in figure 3. It can be seen that there is no substantial difference between cases 3 and 4. Thus, case 3 with 2055 meshes is selected in this study to save computational costs. The chemical reactions are not activated at this stage since this study focuses firstly on the capability of CFD model to simulate multiphase flow dynamics in the fluidized bed reactor. Figure 4 outlines the volume fraction of biomass inside the reactor to 160 s. These results are mapped and initialized for a more advanced simulation with the chemical reactions.

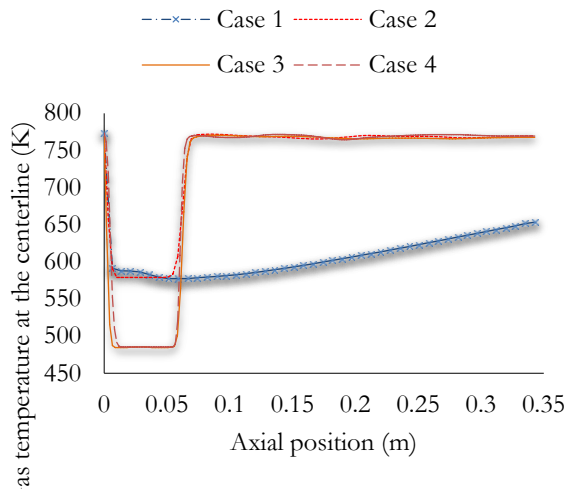


Figure 3. Axial distribution of gas temperature at statistically steady state condition using different grid sizes (no chemical reactions).

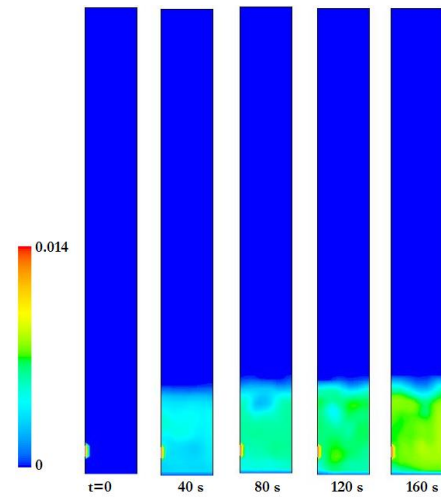


Figure 4. Snapshots of biomass volume fraction (no chemical reactions)

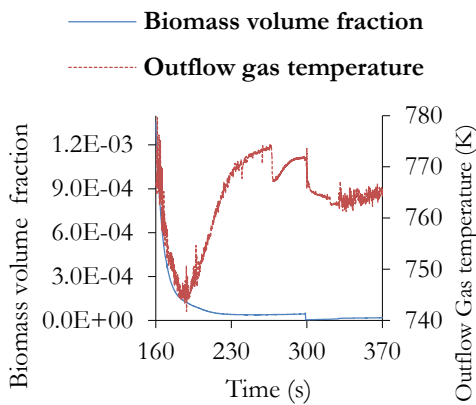


Figure 5. Temporal evolution of area-weighted average of biomass volume fraction and gas temperature at the reactor outlet

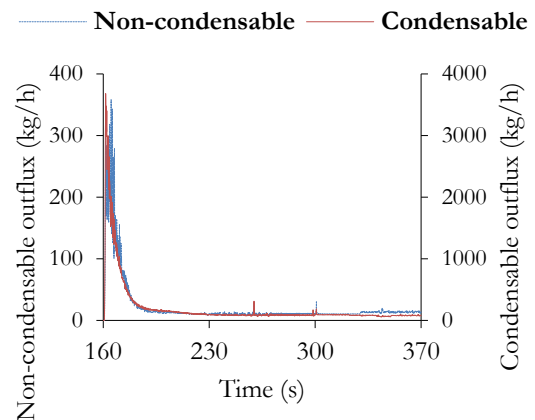


Figure 6. Temporal evolution of non-condensable and condensable outflux

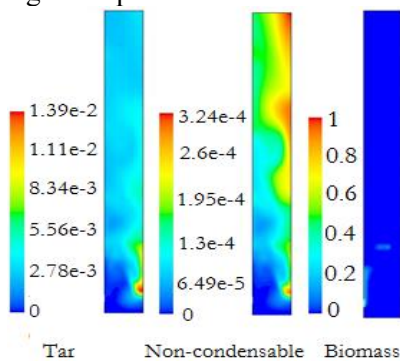


Figure 7. Mass fraction distribution at steady state condition

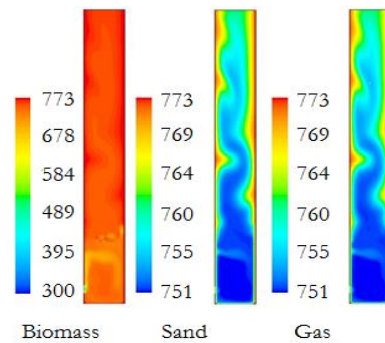


Figure 8. Contour plots of temperature for biomass, gas, and sand at statistically steady state.

In order to obtain a statistically steady state condition, area-averaged biomass volume fraction, outflow gas temperature, tar and non-condensable flows are monitored. Figures 5 and 6 show the temporal evolution of biomass volume fraction, the outflow gas temperature, non-condensable and tar outflux, respectively. It can be seen that all of the values reach statistically steady state condition after $t=330$ s. By monitoring the outflux of the products, the yield of tar, non-condensable, and bio-char in the last 40 seconds, are obtained. By integrating the flow of the product at the reactor outlet, the total mass flow rate of each species during the pyrolysis process is obtained. During the process, tar and non-condensable are added to the gas phase whereas biochar remains in the biomass phase. The mass fractions of products are shown in figure 7 at statistically steady state condition. Tar will be cracked into non-condensable as the temperature increases. Snapshots of temperature for the different phases are illustrated in figure 8. It is observed that except for lower temperatures at the biomass inlet due to cold virgin biomass, temperatures in other regions are in the range of 751-773 K.

Figure 9 illustrates the volume fraction of sand phase after reaching statistically steady state condition. The formation of bubbles in the mixing zone of the reactor is due to the flow of nitrogen as a fluidizing gas from the bottom of the reactor and entrained biomass from the left side of the reactor. These formations of bubbles enhance the gas-solid mixing and consequently facilitate the heat transfer from hot sand and gas and heated wall to the biomass particles. Hence, the required heat for the process is conveniently supplied.

The comparison of product yield against published experimental data [10] is shown in Table 3. As it can be seen, the predicted products yield match the experimental data very well.

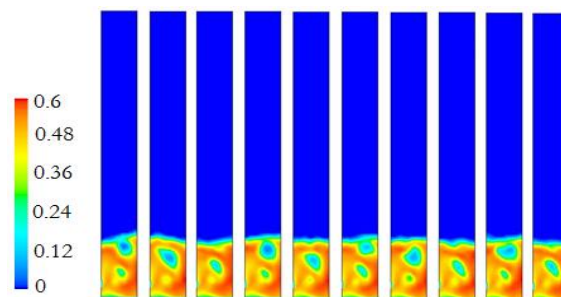


Figure 9. Snapshot of sand volume fraction at statistically steady state condition ($t > 340$ s). The first snapshot on the left is at $t=340.1$ s and the interval between the snapshots is 0.1 s.

Table 3. Comparison of product yield (wt %) between simulation and experiment

Components	Tar	Non-condensable	Biochar
Experiment [10]	82.1	12.4	2.2
Current study	77.8	13.8	2.4

4. Conclusion

In this study, a numerical framework for simulation of fast pyrolysis process is developed. In order to verify the capability of this numerical framework, a standard 2-D lab scale bubbling fluidized bed is selected due to its simplicity and applications. In this simulation, the multi-fluid model with a gas phase and two solid phases are studied. Multiple species are available in each phase. To implement the chemical reactions, the global reaction mechanisms are considered. A list of mathematical formulations for the governing equations is tabulated. The simulated results show an acceptable level of agreement with the published experimental data. It is concluded that the provided numerical framework can predict different properties such as volume fractions, temperatures, velocity, and above all, the product yield of the process accurately. This numerical framework can be applied to more complex geometries for further applications.

References

- [1] Panwar N, Kothari R, Tyagi V 2012 Thermo chemical conversion of biomass–Eco friendly energy routes, *Renewable and Sustainable Energy Reviews*, **16** 1801-1816.
- [2] Goyal H, Seal D, Saxena R 2008 Bio-fuels from thermochemical conversion of renewable resources: a review, *Renewable and sustainable energy reviews*, **12** 504-517.
- [3] Balat M, Kirtay E, Balat H 2009 Main routes for the thermo-conversion of biomass into fuels and chemicals. Part 1: Pyrolysis systems, *Energy Conversion and Management*, **50** 3147-3157.
- [4] Xiong Q, Aramideh S, Kong S C 2014 Assessment of devolatilization schemes in predicting product yields of biomass fast pyrolysis, *Environmental Progress & Sustainable Energy*, **33** 756-761.
- [5] Mellin P, Kantarelis E, Yang W 2014 Computational fluid dynamics modeling of biomass fast pyrolysis in a fluidized bed reactor, using a comprehensive chemistry scheme, *Fuel*, **117** 704-715.
- [6] Papari S, Hawboldt K, Helleur R 2017 Production and Characterization of Pyrolysis Oil from Sawmill Residues in an Auger Reactor, *Industrial & Engineering Chemistry Research*, **56** 1920-1925.
- [7] Xiong Q, Kong S C, Passalacqua A 2013 Development of a generalized numerical framework for simulating biomass fast pyrolysis in fluidized-bed reactors, *Chemical Engineering Science*, **99** 305-313.
- [8] Xiong Q, Aramideh S, Kong S C 2013 Modeling effects of operating conditions on biomass fast pyrolysis in bubbling fluidized bed reactors, *Energy & Fuels*, **27** 5948-5956.
- [9] Bradbury A. G., Sakai Y., Shafizadeh F. 1979 A kinetic model for pyrolysis of cellulose, *Journal of Applied Polymer Science*, **23** 3271-3280.
- [10] Xue Q, Heindel T, Fox R 2011 A CFD model for biomass fast pyrolysis in fluidized-bed reactors, *Chemical Engineering Science*, **66** 2440-2452.
- [11] Gidaspow D 1994 *Multiphase flow and fluidization: continuum and kinetic theory descriptions*, Academic press, Department of Chemical Engineering, Illinois Institute of Technology, Chicago, Illinois.
- [12] Lathouwers D, Bellan J 2001 Yield optimization and scaling of fluidized beds for tar production from biomass, *Energy & Fuels*, **15** 1247-1262.